

NBSIR 75-975

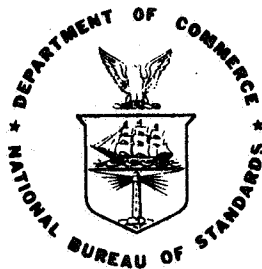
The Calibration of an Optical Flat by Interferometric Comparison to a Master Optical Flat

Charles P. Reeve

Institute for Basic Standards
National Bureau of Standards
Washington, D. C. 20234

December 1975

Final



**U S. DEPARTMENT OF COMMERCE
NATIONAL BUREAU OF STANDARDS**

NBSIR 75-975

**THE CALIBRATION OF AN OPTICAL
FLAT BY INTERFEROMETRIC
COMPARISON TO A MASTER
OPTICAL FLAT**

Charles P. Reeve

Institute for Basic Standards
National Bureau of Standards
Washington, D. C. 20234

December 1975

Final

U.S. DEPARTMENT OF COMMERCE, Rogers C. B. Morton, *Secretary*
James A. Baker, III, *Under Secretary*
Dr. Betsy Ancker-Johnson, *Assistant Secretary for Science and Technology*
NATIONAL BUREAU OF STANDARDS, Ernest Ambler, *Acting Director*

Contents

	Page
1. Introduction -----	1
2. Preliminaries -----	1
2.1. Physical Properties -----	1
2.2. "One-dimensional" Flatness -----	2
2.3. Choice of Profile Reference Line -----	2
3. Geometrical Model for 2-flat Comparison -----	4
3.1. Method of Support -----	4
3.2. Coordinate System -----	7
3.3. Gravitational Bending -----	7
4. Some Results of 3-flat Comparisons -----	7
4.1. Calibration of NBS Master Flats -----	7
4.2. Empirical and Theoretical Bending -----	9
5. Measurement Process -----	11
5.1. Calibration Facilities -----	11
5.2. Choice of Master Flat and Support Radii -----	11
5.3. Preparation for Measurement -----	13
5.4. Procedure for Taking Data -----	13
5.5. Mathematical Model of Fringe Profile -----	15
5.6. Computation of Test Flat Profile -----	19
5.7. Error Analysis -----	24
6. Graphical Display of Profiles -----	26
7. Example -----	27
8. Conclusion -----	31
Acknowledgement -----	33
Table A -----	34
Table B -----	35
References -----	36

The Calibration of an Optical Flat

by Interferometric Comparison to a Master Optical Flat

by

Charles P. Reeve

1. Introduction

The Dimensional Technology Section has been involved in the calibration of optical flats for many years. Present facilities are capable of handling any flat whose diameter does not exceed 16 inches. All test flats are calibrated by either the "2-flat method" or the "3-flat method". The former method is a direct comparison of the test flat to an NBS master flat whose surface profile is well known. The latter method involves an intercomparison between three flats, none of whose profiles need be known. Most test flats are calibrated by the 2-flat method because it is simpler and requires fewer measurements. The 3-flat method is used only for the calibration of NBS master flats or for special calibrations.

The purpose of this report is to present a fairly detailed description of the procedures used in calibrating an optical flat by the 2-flat method. Emphasis is on the geometrical aspects of the setup, the method of obtaining data, the mathematics of data reduction, and the display of the computed results. Some useful results from previous 3-flat calibrations are also incorporated.

2. Preliminaries

2.1. Physical Properties

Normally an optical flat is used in the laboratory as a reference plane in connection with some measurement process. The flat is disc-shaped with parallel or nearly parallel surfaces, one or both of which are of finished optical quality (within a few microinches of flatness except for dubbing at the edges). The most common material for an optical flat is fused quartz, but many are made of glass or one of the newer materials which has a very small coefficient of thermal expansion.

The surface of a fused quartz flat reflects only about 3% of the incident light, so the surface is often coated to give a higher reflec-

tivity. Depending on the type and thickness of the coating, reflectivity can be increased to nearly 100%. A flat with such a highly reflective coating is usually referred to as a mirror. In defining the point where a flat becomes a mirror, use is made of the fact that the closer the reflectivity of two interfering surfaces, the more distinct the fringes. Thus any coated flat which is too reflective to give usable fringes, in the judgement of the observer, against an uncoated master flat is considered to be a mirror and must be calibrated against a coated master flat.

Most flats have two perpendicular diameters which are identified as A-B and C-D by markings on the side. On a one-sided flat the finished surface is indicated and on a two-sided flat the surfaces are usually identified as 1 and 2 or T and B.

2.2. "One-dimensional" Flatness

The objective of the 2-flat method is to measure the profile of the test flat along the specified diameters. This is accomplished by individually comparing each test flat diameter to the known diameter of the appropriate master flat. The measurement process yields an estimated profile for each diameter of the test flat in the form of a discrete number of points $(x_1, y_1), \dots, (x_n, y_n)$ where x_i denotes a position along the diameter and y_i denotes the measured deviation of the surface from some reference line at the position x_i . A sample set of points is given in figure 2.1 where $n=7$. The set of n points corresponding to a given diameter may be plotted and connected by a smooth curve to give a perspective of the measured profile along that diameter as shown in figure 2.2.

Although the surface of an optical flat is often used as a two-dimensional reference plane, it is not calibrated in the two-dimensional sense by the method described herein. This method is most accurately described as a "one-dimensional" flatness measurement with the y_i values being reported as "deviations from a straight line".

2.3. Choice of Profile Reference Line

The choice of which reference line to use in reporting deviations is arbitrary. A set of deviations relative to one straight line can easily be converted to deviations from another. Several definitions of the reference line have been used at the National Bureau of Standards in recent years. Some of these methods of defining the reference line and reporting deviations are:

MEASURED VALUES OF OPTICAL FLAT PROFILE

i	x_i	y_i
1	.06	+ 0.10
2	1.00	1.81
3	2.00	2.79
4	2.50	3.20
5	3.00	3.05
6	4.00	2.89
7	4.94	2.90

Figure 2.1

PLOT OF PROFILE VALUES CONNECTED BY A SMOOTH CURVE

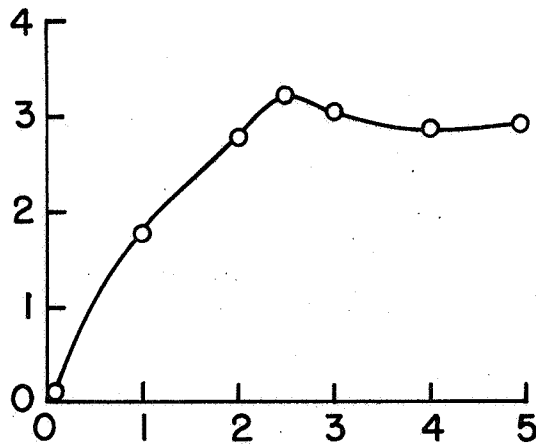


Figure 2.2

(1) If the profile appears to be simply convex or concave let the reference line pass through the end values, and if the deviation of the center value from the line is "d", then report the profile to be "d" microinches convex or "d" microinches concave, depending on the direction of the curvature (fig. 2.3).

(2) Let the reference line pass through the end values and report the deviations from this line (fig. 2.4).

(3) Let the reference line pass through the end values, translate it so that it passes through the center point, and report deviations from this line (fig. 2.5).

(4) Fit a "least squares" line through all values (with the possible exception of the end values) and report deviations from this line (fig. 2.6).

The first method is no longer used because it has the overtones of being a certification rather than a calibration. The last three methods report the measured profile relative to different lines, but they all provide the same information. One cannot say that one reference line is more correct than another. They are all arbitrary and interchangeable. The fourth method, however, is now being used because all measured values have some weight in determining the reference line, and therefore an outlying measurement at some point would have a minimal effect on the deviations from the line at other points.

3. Geometrical Model for 2-Flat Comparison

3.1. Method of Support

When a given diameter of the test flat is compared to the known master diameter one flat is placed horizontally on top of the other so that the two diameters are adjacent and lie in the same vertical plane as shown in figure 3.1. The lower flat is supported on three thin pads which are equidistant from each other. Two of the pads lie on a line parallel to the test diameter. Let the distance from each pad to the center be denoted by $k_L r_L$, where r_L is the radius of the lower flat and k_L is a constant between zero and one. Similarly, the upper flat is supported on the lower flat by three thin pads, each at a distance of $k_U r_U$ from the center of the upper flat. These three pads are also equidistant and have the same orientation as the pads supporting the lower flat. The pad farthest from the diameter (indicated by +) is slightly thicker than the other two so that the air space between the flats is wedge-shaped. The constants k_L and k_U are chosen in a way that will maximize the effectiveness of the measurement system. Guidelines for determining these parameters are discussed later.

"d" MICROINCHES CONVEX

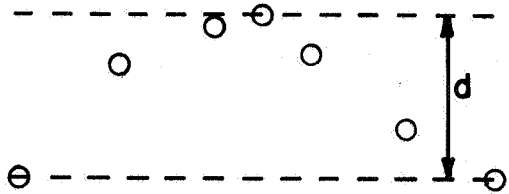


Figure 2.3

$y_1 = y_7 = 0$

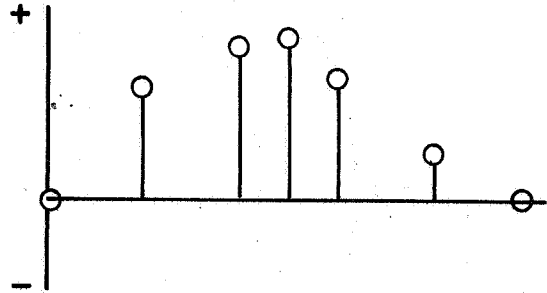


Figure 2.4

$y_4 = 0$ $y_1 = y_7$

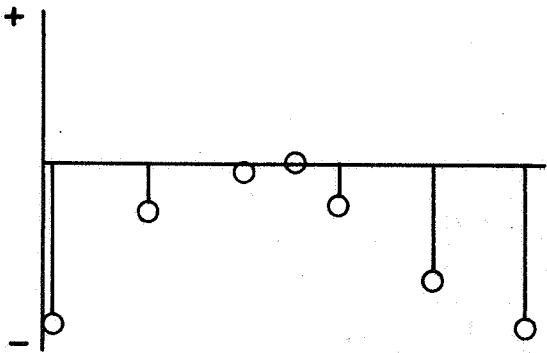


Figure 2.5

Least squares line does not include end points

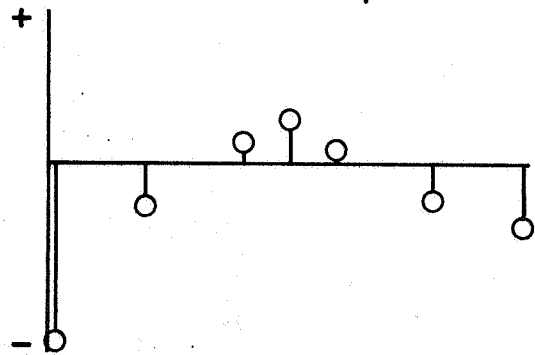


Figure 2.6

2-FLAT SETUP

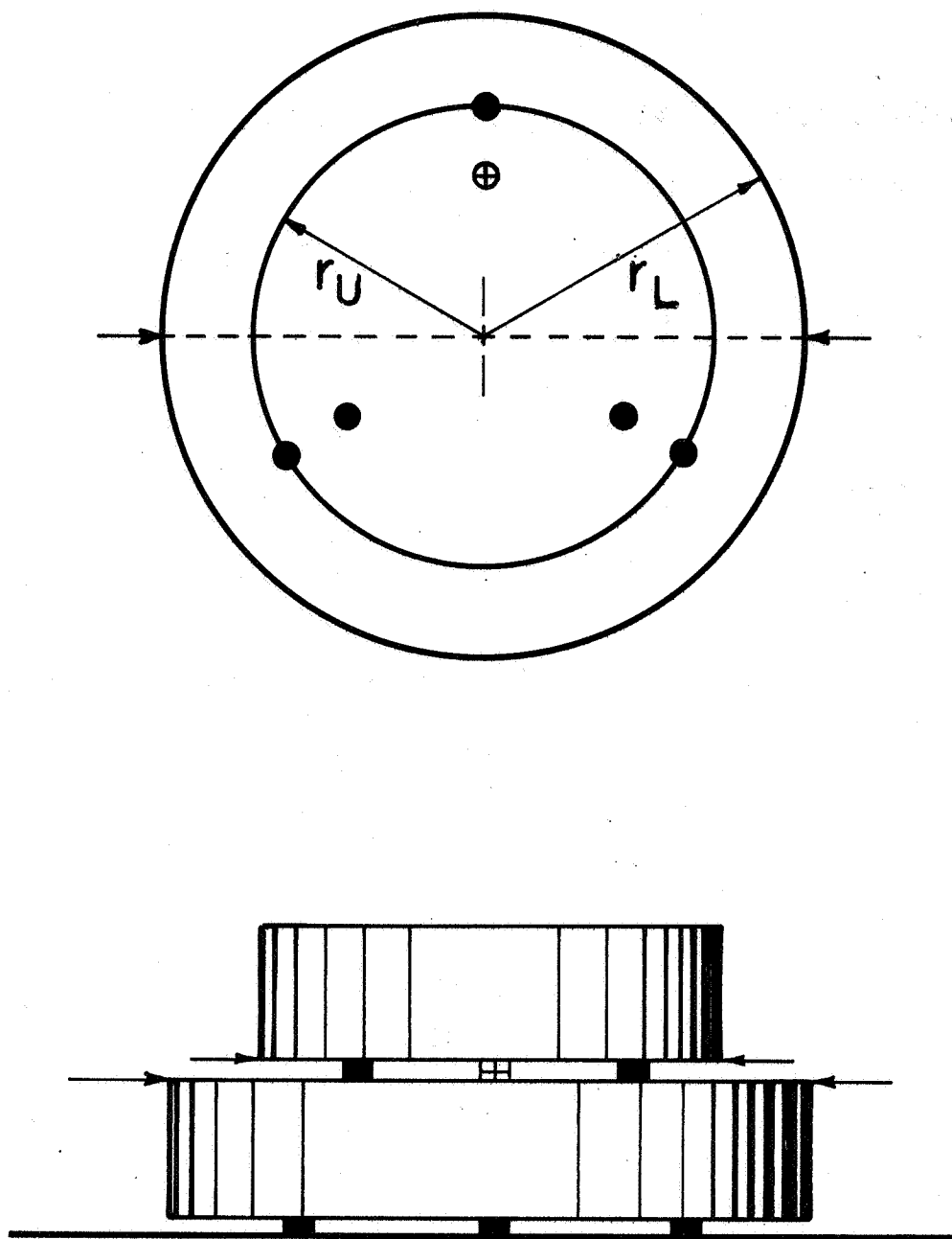


Figure 3.1

3.2. Coordinate System

It is necessary to assign a coordinate system to each diameter of the test flat for the purpose of identifying points along the diameter at which measurements of the surface profile are to be made. Readings are taken at n positions along each diameter where n is usually odd. These positions are denoted by (x_1, \dots, x_n) and are usually symmetrically spaced about the center point at inch or half-inch intervals. If the end positions fall at the extreme edge of the flat they are moved one-sixteenth of an inch toward the center. The positions are usually chosen to coincide with those used in previous calibrations. If the flat has not previously been calibrated the positions are chosen as deemed appropriate. The x_1 position is at the A end of the A-B diameter and the C end of the C-D diameter, and the x_n position is at the B and D ends respectively.

3.3. Gravitational Bending

The freeform profile of an optical flat is defined as that form which the flat would take in a zero-gravity environment. Since no such environment yet exists in earthbound laboratories the distortion of optical flats by gravitational bending must be considered.

When a flat is supported on three pads, the test diameter will have an apparent profile (a) which is the sum of its freeform profile (f) and its bending profile (b). The bending profile is dependent on the support radius of the pads and whether the diameter is on the top or bottom surface of the flat. Many years ago Emerson [4]* showed experimentally that when the support radius of the pads is set so that minimum bending occurs, then the bending is small enough to be neglected. This result is discussed in section 4.2. The current calibration process calls for all test flats and most master flats to be supported at the minimum bending radius. The exception is discussed in section 5.2.

4. Some Results of 3-Flat Comparisons

Although the 3-flat method has not been described in detail, it has been used to give some important results which are relevant to the functioning of the 2-flat method. These results fall into two groups.

4.1. Calibration of NBS Master Flats

The 3-flat method is ideal for calibrating master flats because it

* Figures in brackets indicate literature references listed at the end of this paper.

RING SUPPORT AT EDGE

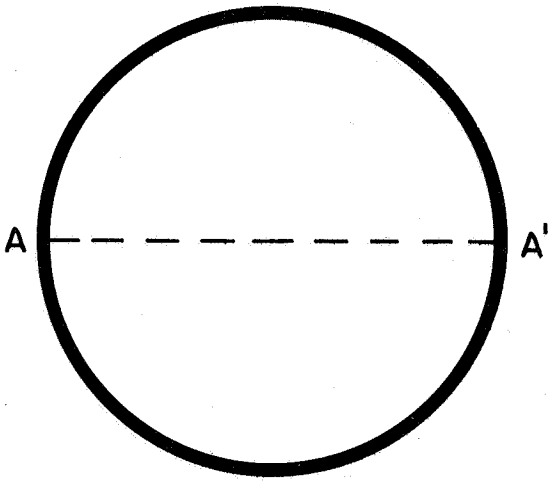


Figure 4.1

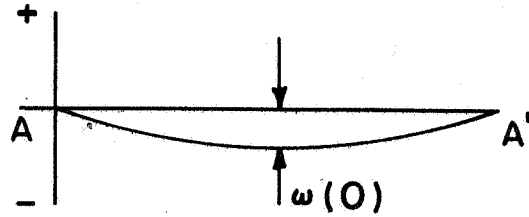


Figure 4.2

THREE POINT SUPPORT AT EDGE

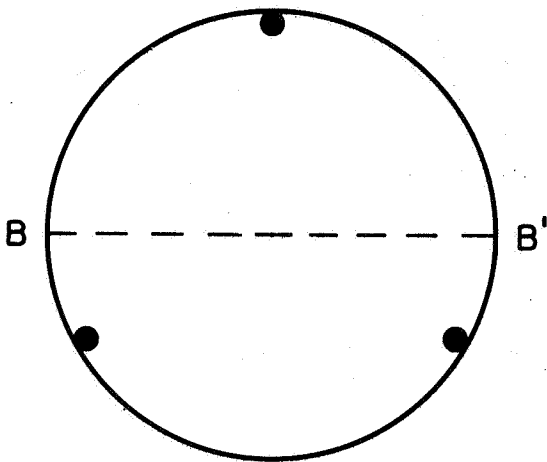


Figure 4.3

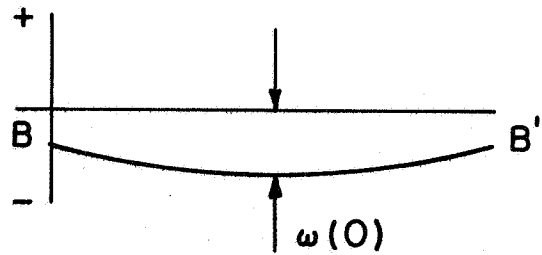


Figure 4.4

gives an "absolute" calibration. No master values are needed and the process is relatively free of systematic errors. The measurement scheme is such that the bending profiles are removed leaving only the freeform profiles. The more commonly used masters are recalibrated by this method occasionally to check on their stability.

4.2. Empirical and Theoretical Bending

In 1950 and 1954 three 10.6 inch master flats (designated #1-1, #1-2, and #1-3) were involved in a thorough study headed by Emerson[4] where the profiles and bending characteristics of the flats were measured. Bending profiles of flat #1-3 were determined for six different support radii. Currently this is the only NBS master flat for which experimentally derived bending corrections exist.

One result of the bending research was the discovery that minimum bending along the test diameter occurs when the support pads are located at $.70r$ from the center. This result is not surprising since the circle of radius

$$r_0 = \frac{r}{\sqrt{2}} = .7071r$$

divides the mass of the flat into equal parts. The bending corrections for the $.70r$ support were found to be negligible for the 10.6 inch flat, so it is usually assumed that when flats of this size or smaller are supported at $.70r$ the bending is negligible and the apparent profile is the same as the freeform profile.

Some theoretical bending values have been developed by Timoshenko[5] for circular flats using the following two types of support:

I. Ring support at the edge

Figures 4.1 and 4.2 show a flat supported at the edge by a narrow ring and the corresponding profile of diameter AA'. On the diameter AA', a distance r from the center, the bending deflection or sag $w(r)$ is given by the formula

$$w(r) = \frac{3\rho g(1-\nu^2)(a^2-r^2)}{16Eh^2} \left[\frac{(5+\nu)}{(1+\nu)} * a^2 - r^2 \right] + \frac{\rho g}{4E} (3+\nu)(a^2 - r^2) \quad (4-1)$$

where: a = radius (in.)
 h = thickness (in.)
 ν = Poisson's ratio (dimensionless)
 ρg = density (lb./in.³)
 E = Young's modulus (lb./in.²).

Note that if the ratio a/h is large, then the first term greatly exceeds the second, so $w(r)$ can then be considered inversely proportional to the square of the thickness.

Example. For NBS master flat #1-3, $a = 5.3$, $h = 2.5$, $\nu = 0.14$, $E = 10.15 \times 10^6$, and $\rho g = .079876$. By letting $r = 0$, the sag at the center relative to the ring support is computed to be

$$w(0) = .823 + .174 = .997 \text{ microinches.}$$

Note that $w(a) = 0$.

II. Three point support at the edge

Figures 4.3 and 4.4 show a flat supported at the edge on three points and the corresponding profile of diameter BB' . The formula for the bending deflection is given only for $r = 0$ as

$$w(0) = .0362 \frac{Pa^2}{D} \quad (4-2)$$

where $P = \pi a^2 q$, $D = Eh^3/12(1-\nu^2)$, and $q = \rho gh$. Combining terms then

$$w(0) = \frac{1.3647 \rho g (1-\nu^2) a^4}{Eh^2} \quad (4-3)$$

Example. For NBS master flat #1-3, using the same values as before,

$$w(0) = 1.329 \text{ microinches.}$$

The value $w(a)$ for the second example is obviously not equal to zero but since the formula given is only for $r = 0$ it is unclear how to determine the deflection for values of r different from zero. Consequently, it is impossible to directly compare this theoretical bending value with the observed bending value obtained by Emerson.

These two theoretical formulae, though interesting, have little or no application to the current measuring process. Only by making certain gross assumptions could they be applied and at the present time it is felt that such assumptions cannot be justified.

The conclusion of this section then is that when an optical flat is being used as a master it should be supported at $.70r$ where bending is assumed to be negligible. It should be supported at another radius only when experimentally obtained bending values have been established. In

that case the apparent profile of the master is computed by adding or subtracting (whichever is appropriate) the bending profile to (or from) the freeform profile.

5. Measurement Process

5.1. Calibration Facilities

The current optical flat calibration facilities are located in a laboratory which is maintained at a constant temperature of 20° Celsius and at a near constant humidity. In order to keep the temperature stable during the measurement process, only the person who is making the measurements is allowed in the room. It is certain that thermal gradients do exist within the optical flats, but it is assumed that they are small enough in magnitude to be neglected; therefore, no attempt is made to correct for temperature. It is also known that the daily variation in atmospheric pressure affects the wavelength of light, but this effect is negligible because only small differences in profile are measured.

The master and test flat assembly is encased in a cardboard and aluminum foil insulating shell and is set on ways which allow it to pass back and forth under a Pulfrich viewer as shown in figures 5.1 and 5.2. The maximum travel on the ways is slightly more than 16 inches.

5.2. Choice of Master Flat and Support Radii

In determining the best setup to use for calibrating a given test flat, the following facts must be considered:

- (1) The test flat must be supported at seven-tenths of its own radius.
- (2) The master flat must be supported at seven-tenths of its own radius unless its bending corrections are known.
- (3) Due to bending considerations it is best to have the heavier flat on the bottom.
- (4) If the weight of the upper flat will significantly bend the lower flat then the support pads for the upper flat must be directly above the support pads for the lower flat.
- (5) NBS master flat #1-3 may be supported anywhere from $.25r_M$ to $1.00r_M$ if bending corrections are properly applied.

The guidelines in table A have evolved from these considerations.

TOP VIEW OF CALIBRATION SETUP

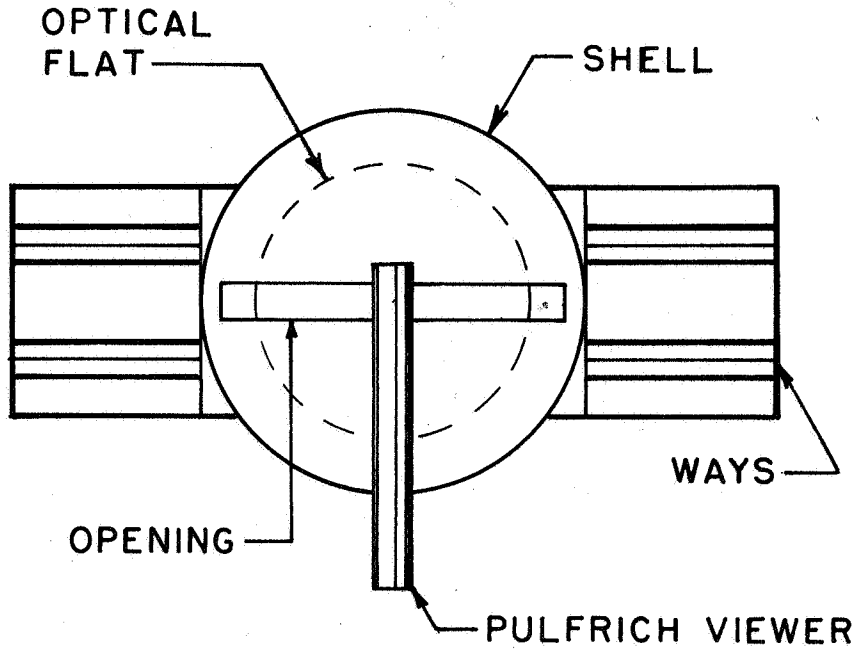


Figure 5.1

DIAGRAM OF INTERFEROMETER

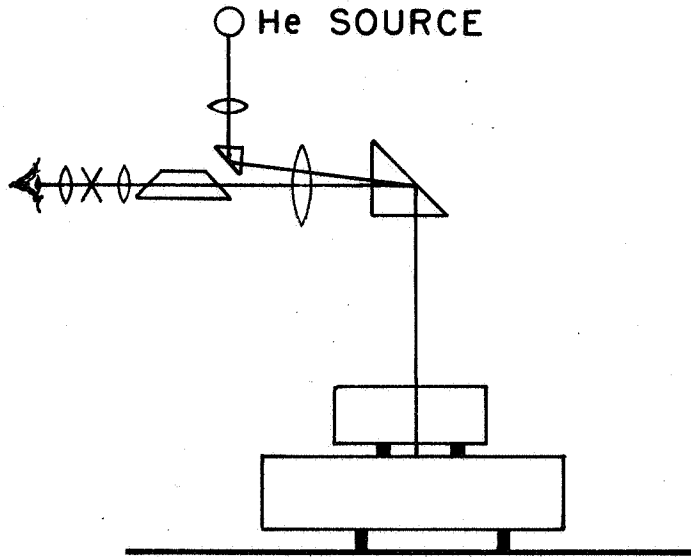


Figure 5.2

5.3. Preparation for Measurement

When two flats are set up for measurement, the alignment of the assembly should be checked to be sure that the test diameter passes back and forth directly under the viewer. When the lamp is turned on a series of interference fringes will be observed running roughly parallel to the diameter. It is desirable that these fringes be as nearly parallel to the diameter as possible. A slight angular movement of the fringes can be obtained by pressing lightly over one of the thin pads. It is then very important to check the direction of the wedge by pressing lightly over the thicker pad. This should make the fringe separation wider. If the fringe separation becomes narrower it indicates that the "thick" pad is actually thinner than the thin pads, and the resulting sign reversal will create errors in the computed values of the profile. This method of increasing the fringe separation also spreads out the dark fringes and makes them fuzzier. By controlling the thickness of the pads the dark area of the fringe can be made just the right width to fit between the crosshairs of the viewer. For helium yellow light and the Pulfrich viewer the ideal distance between fringes is 200-300 micrometer units or 2.2-3.3 millimeters.

The points along the diameter at which measurements are to be made are located with the aid of a paper ruler which has notches cut at the proper x positions. The ruler is laid on top of the upper flat along side the test diameter so that it appears with the fringes in the viewer as shown in figure 5.3.

After all preparations have been completed the flats are allowed to sit for several hours, or preferably overnight, so that they come to thermal equilibrium. It is likely that during this time there will be a slight angular and lateral movement of the fringes. This is allowable because the effect of these changes is removed by the data reduction process.

5.4. Procedure for Taking Data

The fringe which most nearly coincides with the test diameter is chosen as the primary fringe (fig. 5.4). The y position of this fringe is measured at designated points along the diameter. Beginning at the position x_1 the crosshairs are moved by a micrometer dial until they are centered over the primary fringe (fig. 5.3). The dial reading y_1 is recorded. The assembly is then moved by the hand crank until the position x_2 is centered under the viewer and the crosshairs are again centered over the fringe. The reading y_2 is recorded. This process is repeated until readings at all n positions have been made. Then, without delay, the measurements are repeated in reverse order so that a series of $2n$ measurements of the

INTERFERENCE FRINGES

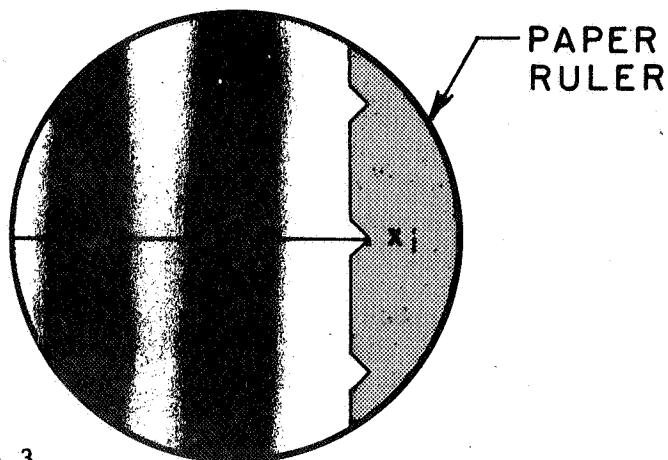


Figure 5.3

PRIMARY FRINGE



Figure 5.4

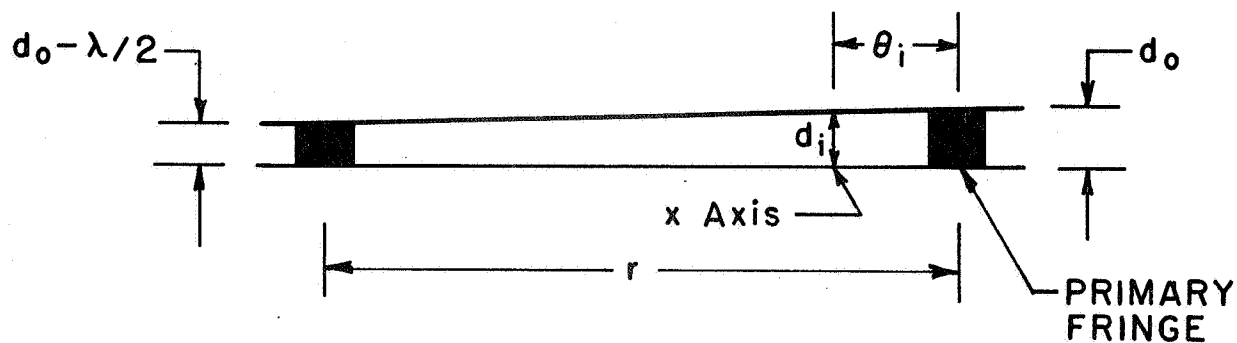


Figure 5.5

fringe profile is generated. Depending on the value of n , the measurements may take up to 30 minutes to complete. These measurements can then be said to constitute one cycle of data. The usual procedure is to take one to four cycles of data at a time which constitutes a run. Directly before and after each run several measurements of the distance between the primary fringe and one of the two adjacent fringes are made. This distance is called the fringe separation and is denoted by " r ". Two independent runs are made per diameter. It is desirable for these runs to be at least two hours apart in order to test the stability of the fringe pattern.

5.5. Mathematical Model of Fringe Profile

In setting up a mathematical model for a run it is necessary to consider that the fringes may drift significantly during the course of the run and the observer may need to take a break of variable length between cycles. The model which follows accounts for these factors. Within each cycle the measurements should be equally spaced in time and completed as quickly as possible. Over this period the fringe drift is assumed to be linear. Between cycles the observer may take a break because nothing is assumed about the behavior of the fringes over that period of time. The entire run, however, should be completed within a couple of hours if possible in order to reduce the number of long-term variations which might arise.

Assume that within a cycle the measurements are spaced by two units of time, and for the sake of symmetry let the time $t=0$ fall halfway between the consecutive measurements at the x_n position. At $t=0$ during the first cycle let the distance from the position x_i on the test diameter to the fringe be given by θ_i as shown in figure 5.6. (The fringes are shown as straight lines for simplicity.) The purpose of the model then is to estimate these values θ_i where $i=1,n$. At times before and after $t=0$ the fringe position will drift, as shown by the dotted lines, and the distance to the fringe will change. This change can be modeled by assuming that at each end point the fringe has a constant drift throughout the cycle. Let b_j denote the rate of movement of the fringe in micrometer units per unit time at the x_i position during the j^{th} cycle, and let d_j similarly denote the rate of movement of the fringe at the x_n position. The movement of the fringe at the x_i position is then a weighted average of the end effects with the weighting function depending on x_i .

Irregular jumps in the fringe position between cycles can easily be modeled. Let a_j be the distance the fringe moves at the x_i position be-

**FRINGE DRIFT DURING CYCLE 1 AND
FRINGE JUMP BETWEEN CYCLES 1 & 2**

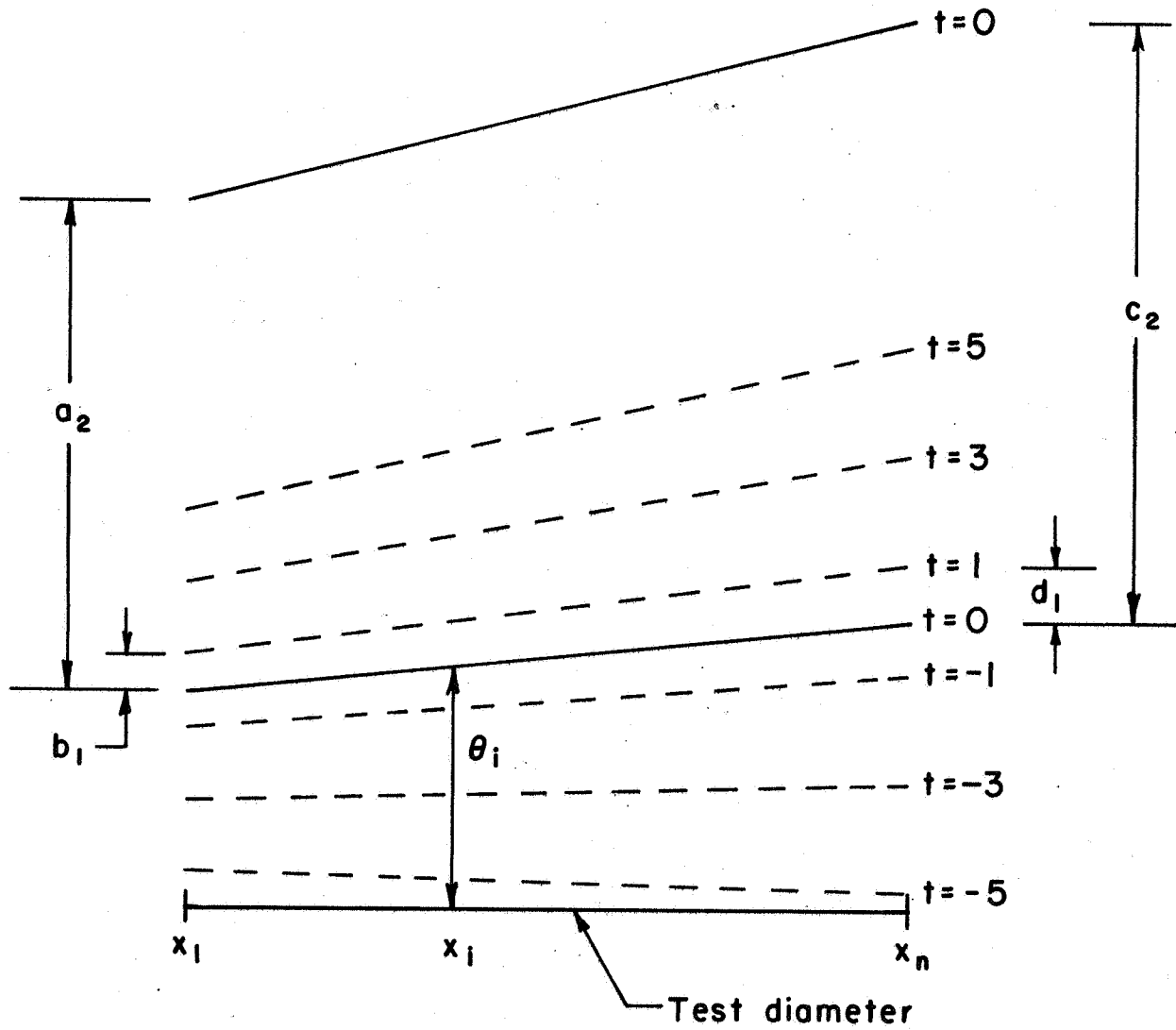


Figure 5.6

tween $t=0$ for the first cycle and $t=0$ for the j^{th} cycle as shown in figure 5.6. Let c_j similarly denote the distance the fringe has moved at the x_n position, and note that $a_1=c_1=0$. Again the movement of the fringe at the x_i position is a weighted average of the end effects. Let m be the number of cycles per run and let y_{ij} be the i^{th} observation in the j^{th} cycle. Then the measurement equations take the form

$$y_{ij} = \theta_i + [a_j + b_j(2i-2n-1)] \left[\frac{x_n - x_i}{x_n - x_1} \right] + [c_j + d_j(2i-2n-1)] \left[\frac{x_i - x_1}{x_n - x_1} \right] + \epsilon_{ij} \quad \text{if } 1 \leq i \leq n, \text{ and} \quad (5-1)$$

$$y_{ij} = \theta_{2n-i+1} + [a_j + b_j(2i-2n-1)] \left[\frac{x_n - x_{2n-i+1}}{x_n - x_1} \right] + [c_j + d_j(2i-2n-1)] \left[\frac{x_{2n-i+1} - x_1}{x_n - x_1} \right] + \epsilon_{ij} \quad \text{if } n < i \leq 2n,$$

where $j=1, m$ and the ϵ_{ij} are independent error values from a distribution with mean zero and variance σ^2 .

This linear model can be solved by the usual method of least squares (i.e., minimizing $\sum_{i=1}^{2n} \sum_{j=1}^m \epsilon_{ij}^2$). Let the $2nm$ observations be given by the vector

$$y = (y_{11} \ y_{21} \ \dots \ y_{2n,1} \ \dots \ y_{1m} \ y_{2m} \ \dots \ y_{2n,m})', \quad (5-2)$$

and let the $n+4m-2$ unknowns be given by the vector

$$\begin{pmatrix} \theta \\ \Omega \end{pmatrix} = (\theta_1 \ \theta_2 \ \dots \ \theta_n \ b_1 \ d_1 \ a_2 \ b_2 \ c_2 \ d_2 \ \dots \ a_m \ b_m \ c_m \ d_m)', \quad (5-3)$$

where θ is $n \times 1$ and Ω is $(4m-2) \times 1$. Since $a_1=c_1=0$, they are not included

in the model. Let p , q , u , and v be vectors of order n whose components are given by

$$\begin{aligned}
 p_i &= \frac{x_n - x_i}{x_n - x_1}, \\
 q_i &= 1 - p_i, \\
 u_i &= (2n - 2i + 1)p_i, \text{ and} \\
 v_i &= (2n - 2i + 1)q_i
 \end{aligned}
 \tag{5-4}$$

where $i=1, n$. Let I be the identity matrix of order n and let K be the $n \times n$ matrix with 1's on the minor diagonal and 0's elsewhere, i.e.,

$$K = \begin{bmatrix} 0 & 0 & \dots & 0 & 1 \\ 0 & 0 & & 1 & 0 \\ \vdots & & \ddots & & \\ 0 & 1 & & 0 & 0 \\ 1 & 0 & & 0 & 0 \end{bmatrix}.
 \tag{5-5}$$

(Note that premultiplication of an $n \times 1$ vector by K flips the vector.) Let the $2nm$ residuals be given by the vector

$$\epsilon = (\epsilon_{11} \ \epsilon_{21} \ \dots \ \epsilon_{2n,1} \ \dots \ \epsilon_{1m} \ \epsilon_{2m} \ \dots \ \epsilon_{2n,m})',
 \tag{5-6}$$

and let the $(2nm) \times (n+4m-2)$ matrix of coefficients be given by

$$X = \begin{bmatrix} I & -u & -v & 0 & 0 & 0 & 0 & 0 & 0 & 0 & 0 \\ K & Ku & Kv & 0 & 0 & 0 & 0 & 0 & 0 & 0 & 0 \\ I & 0 & 0 & p & -u & q & -v & 0 & 0 & 0 & 0 \\ K & 0 & 0 & Kp & Ku & Kq & Kv & 0 & 0 & 0 & 0 \\ \vdots & & & & & & & & & & \\ I & 0 & 0 & 0 & 0 & 0 & 0 & p & -u & q & -v \\ K & 0 & 0 & 0 & 0 & 0 & 0 & Kp & Ku & Kq & Kv \end{bmatrix}$$

The measurement equations are then given by

$$y = X \begin{pmatrix} \theta \\ \Omega \end{pmatrix} + \epsilon
 \tag{5-8}$$

The least squares estimation takes the form

$$E(y) = X \begin{pmatrix} \theta \\ \Omega \end{pmatrix} \text{ where} \quad (5-9)$$

$$\text{Var}(y) = \sigma^2 I .$$

The normal equations are given by

$$X'X \begin{pmatrix} \theta \\ \Omega \end{pmatrix} = X'y \quad (5-10)$$

and the estimates are given by

$$\begin{pmatrix} \hat{\theta} \\ \hat{\Omega} \end{pmatrix} = (X'X)^{-1} X'y = \begin{pmatrix} V & U \\ U' & W \end{pmatrix} X'y \quad (5-11)$$

where V is nxn, U is nx(4m-2), and W is (4m-2)x(4m-2). The predicted values of the observations are given by

$$\hat{y} = X \begin{pmatrix} \hat{\theta} \\ \hat{\Omega} \end{pmatrix} \quad (5-12)$$

and the deviations by

$$d = y - \hat{y} . \quad (5-13)$$

The estimate of σ is given by

$$s = \sqrt{d'd / (2nm - n - 4m + 2)} . \quad (5-14)$$

(At this point the above parameters are expressed in micrometer units.)

In summary, the results of this fitting procedure which are of primary interest are the set of n estimated fringe positions, $\hat{\theta}_i$, and the estimated standard deviation of a single measurement, s.

5.6. Computation of Test Flat Profile

Each estimated fringe profile is now converted to an estimate of the air space between the flats along the given diameter. Figure 5.5 shows a cross section of the setup which is cut perpendicular to the x axis at the position x_i . The separation d_i at the position x_i is related to the fringe profile θ_i by

$$d_i = d_0 - \frac{\lambda \hat{\theta}_i}{2r} \quad (5-15)$$

where d_0 is the separation of the flats along the primary fringe, and λ is the wavelength of the monochromatic light. (The d_i values are now expressed in microinches.) The separation d_i is also related to the profiles of the two flats. Figure 5.7 shows a cross-section of the setup along the test diameter as viewed horizontally with the upper flat being designated U and the lower flat L. For the purposes here it does not matter which is the test flat and which is the master. Let r^U and r^L be parallel auxiliary lines separated by an arbitrary distance h which pass through the upper and lower flats respectively, and for each line let the direction toward the other line be the positive direction. The adjacent profiles of the upper and lower flats can then be taken as deviations a_i^U and a_i^L from the lines r^U and r^L respectively. At every position x_i the relation between the parameters takes the form

$$h = a_i^U + a_i^L + d_i. \quad (5-16)$$

Substitution of the expression for d_i in equation 5-15 into equation 5-16 gives the following expression for the sum of the apparent profiles of the two flats:

$$a_i^U + a_i^L = \frac{\lambda \hat{\theta}_i}{2r} + h - d_0. \quad (5-17)$$

The value of h was arbitrary so it may be set equal to d_0 . Then

$$a_i^U + a_i^L = \frac{\lambda \hat{\theta}_i}{2r}. \quad (5-18)$$

Let the vector of profile values $a_i^U + a_i^L$ be denoted by a_I for the first run and a_{II} for the second run. Intuitively, the difference $a_I - a_{II}$ should be linear in x because the flats are rigid bodies. A statistical test is performed under this assumption in order to determine if there is a significant between-run error term. If such a term is found to be significant then the measurement process is said to be "not in control" and the measurements are repeated.

The test is implemented as follows. Let s_I and s_{II} be the respective standard deviations of a single measurement of runs 1 and 2, given in eq-

RELATIONSHIP OF PROFILES

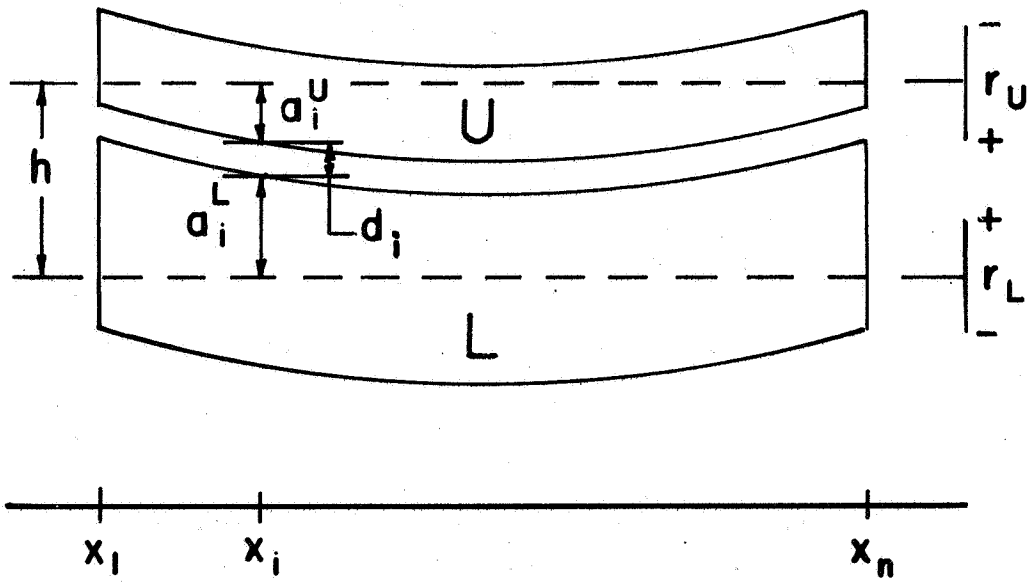


Figure 5.7

uation 5-14, which have been converted to microinches, and let

$$z = a_I - a_{II} \quad (5-19)$$

A constant term α_0 and a linear term α_1 are removed from the vector of z values as follows: Let

$$X = \begin{bmatrix} 1 & x_1 \\ 1 & x_2 \\ \vdots & \vdots \\ 1 & x_n \end{bmatrix} \quad \text{and} \quad \alpha = \begin{pmatrix} \alpha_0 \\ \alpha_1 \end{pmatrix} \quad (5-20)$$

The least squares estimation of α takes the form

$$\begin{aligned} E(z) &= X\alpha \\ \text{and} \\ \text{Var}(z) &= V\sigma_t^2 \end{aligned} \quad (5-21)$$

where V is as given in equation 5-11. The total variance σ_t^2 can be written as

$$\sigma_t^2 = \sigma_w^2 + \sigma_b^2 \quad (5-22)$$

where σ_w^2 is the within-run variance and σ_b^2 is the between-run variance. The estimates $\hat{\alpha}$ are of no importance. The vector of residuals is given by

$$d = z - \hat{z} = [I - X(X'V^{-1}X)^{-1}X'V^{-1}]z, \quad (5-23)$$

and the estimate of the total variance is given by

$$s_t^2 = \frac{d'V^{-1}d}{n-2} \quad (5-24)$$

The within-run variance is estimated by

$$s_w^2 = s_I^2 + s_{II}^2 \quad (5-25)$$

The ratio

$$S = s_t^2/s_w^2 \quad (5-26)$$

has an F distribution with $(n-2, 4nm-2n-8m+4)$ degrees of freedom. Taking the level of significance of the test to be .01, the value

$$F = F_{.99}(n-2, 4nm-2n-8m+4) \quad (5-27)$$

is obtained from table B. If $S > F$ then the between-run error, σ_b^2 , is determined to be significant and the system is "not in control". If $S \leq F$ then the between-run error is determined to be not significant and the mean of the two runs,

$$a = \frac{a_I + a_{II}}{2} \quad (5-28)$$

is computed and separated into components,

$$a = a^T + a^M \quad (5-29)$$

where a^T and a^M are the respective apparent profiles of the test flat and master flat. The master flat profile is subtracted to give

$$a^T = a - a^M \quad (5-30)$$

Recall from section 3.3 that if a bending correction b^M is used in determining a^M , then the sign of b^M depends on whether the master flat is on the top or bottom. If the bending profile of the master flat is unknown then it is usually assumed to be zero provided the master flat is supported at $0.70r_M$.

The computed profile a^T also contains an unknown bending value b^T . If the test flat is used in the orientation opposite the one in which it was calibrated, there will be a difference in the respective apparent profiles of $\pm 2b^T$. This difference can usually be assumed negligible when the flat is supported at $0.70r_T$.

The exact degree of bending in a given flat is highly dependent on its radius and thickness (see section 4.2). There is evidence that flats which are 10" or less in diameter have negligible bending when supported at $0.70r$. For example, when the NBS 10.6" master flat is supported at $0.70r$ the maximum bending along its diameter has been shown experimentally to be 0.02 microinches.

The values a^T given in equation 5-30 are referenced to some arbitrary line. The final profile values a^{*T} which are referenced to the least squares line through the profile must be determined. Frequently the end values of the profile will fall off sharply if measurements

were made near the edge of the flat where there is dubbing. If these values were equally weighted they might distort the appearance of flatness along the diameter. To account for this possibility a diagonal weighting matrix,

$$W = \begin{bmatrix} w_1 & 0 & \dots & 0 & 0 \\ 0 & 1 & & 0 & 0 \\ \vdots & & \ddots & & \\ 0 & 0 & & 1 & 0 \\ 0 & 0 & & 0 & w_n \end{bmatrix} \quad (5-31)$$

is introduced where $w_1 = w_n = 0$ if the end points are in the dubbing and $w_1 = w_n = 1$ if not. Let

$$X_w = WX \quad (5-32)$$

where X is as defined in equation 5-20. The final vector of profile values is then given by

$$a^T = [I - X(X_w' X_w)^{-1} X_w'] a^T = Qa^T \quad (5-33)$$

5.7. Error Analysis

The uncertainty of the computed profile values can be expressed as the sum of random and systematic components of error. The random component is taken to be the three standard deviation limit for random error. The systematic component is taken to be the sum of all other known effects which contribute error to the system.

Let s_p , the pooled standard deviation of a single measurement (in microinches), be estimated from all runs made on the diameters of the test flat. From equations 5-18 and 5-11,

$$\text{Var}(a_I) = \text{Var}(a_{II}) = V s_p^2, \quad (5-34)$$

and

$$\text{Var}(a) = \text{Var}\left(\frac{a_I}{2}\right) + \text{Var}\left(\frac{a_{II}}{2}\right) = V \left(\frac{s_p}{2}\right)^2 \quad (5-35)$$

From equation 5-30,

$$\text{Var}(a^T) = \text{Var}(a) + \text{Var}(a^M) = \text{Var}(a) = V \left(\frac{s_p}{2}\right)^2 \quad (5-36)$$

since the values a^M are constants. From equation 5-33

$$\text{Var}(a^{*T}) = Q [\text{Var}(a^T)] Q' = Q \left[v \left(\frac{s_p^2}{2} \right) \right] Q' = QVQ' \left(\frac{s_p^2}{2} \right), \quad (5-37)$$

therefore the standard deviation of the i^{th} profile value of the test flat is

$$s_{a_i}^{*T} = \sqrt{\frac{(QVQ')_{ii}}{2}} s_p \quad (5-38)$$

Two non-negligible sources of systematic error are the uncertainty of the master flat values and the non-linearity of the ways which move the flats back and forth under the viewer. Let E_M be the largest uncertainty of the master flat values (including bending uncertainties), and let E_W be the maximum error caused by the non-linearity of the ways. For the current setup the ways are believed to be straight to within .0002 inch which corresponds to .47 micrometer units. This error is converted to test flat profile error by

$$E_W = .47 \frac{\lambda}{2r_{\max}} \quad (5-39)$$

where r_{\max} is the maximum fringe separation for all runs on the test flat diameters. All other sources of systematic error are assumed to be negligible; therefore, the limit for total systematic error is

$$E = E_M + E_W \quad (5-40)$$

and the total uncertainty of the computed profile values is

$$U_{a_i}^{*T} = 3s_{a_i}^{*T} + E \quad (5-41)$$

One shortcoming of this calibration process is its lack of strict statistical controls. The test for between-run variance given in section 5.6 is not broad enough to detect all possible errors which might occur. A test of the "computed" standard deviation against an "accepted" standard deviation is not possible since each calibration involves certain factors which make it unique. Two such factors are the fringe sharpness, which varies depending on the fringe separation and the reflective properties of the flats, and the skill of the particular observer in centering the fringe in the crosshairs of the viewer. Over many years these factors

have combined to give standard deviations of a single measurement between .05 and .25 microinches. In the absence of a strict statistical test, the standard deviation is accepted if it lies within this range.

Since there is no check standard in the process, a change in the master values could go undetected until the master itself is recalibrated. To guard against the possibility of such an error the computed profile of the test flat is checked against a previous calibration if one exists. There is strong evidence that no significant long-term change in the profile of master flats occurs when used at a temperature of 20°C. The NBS 10.6 inch master flat, for example, has been calibrated four times over a period of 18 years and the maximum disagreement in values is .13 microinch. This difference is easily within the limits of random measurement error. To assure their stability, all NBS master flats are periodically calibrated by the 3-flat method.

Although most of the above controls are not rigid, they have proven to be adequate for protection against gross errors.

6. Graphical Display of Profiles

Ideally the calibration of an optical flat along a given diameter would yield a continuous curve which represents the profile of the flat along the diameter. Such a calibration could be accomplished under the current measurement system by letting n take on a very large value, but the data-taking process would be quite laborious for the observer. In general, high quality optical flats have smooth profiles which can be adequately represented by measuring the profile at a few points and connecting the points with a smooth curve. In pre-computer days a hand drawn graph of each diameter was sometimes submitted as a supplement to the Report of Calibration. Such a graph was useful in giving the user a good idea of the profile at a glance. The present computer facilities allow a graph of each diameter to be plotted as part of the data reduction process.

One good method of fitting a smooth curve to a discrete set of points involves the use of cubic spline functions. Let the set of points $\{(x_i, a_i), i=1, n\}$ represent the profile of a diameter. In each of the intervals $\{(x_i, x_{i+1}), i=1, n-1\}$ a cubic polynomial is fit to the points subject to the condition that the cubic between points x_{i-1} and x_i must agree with the cubic between points x_i and x_{i+1} at the point x_i in their first and second derivatives. Also, either the first or second derivatives, but not both, must be specified at the end points x_1 and x_n . For this problem it seems most natural to set the second derivatives equal to

zero. The resulting equations form a tridiagonal system of $3n-3$ equations in $3n-3$ unknowns. Methods for formulating and solving this system are given in Ahlberg [1] and UNIVAC [6]. Once the coefficients of the $n-1$ cubics are obtained the interpolated value at a given point x_0 is determined by plugging the value of x_0 into the appropriate cubic.

Interpolated values were computed at 201 equally spaced points for each of the diameters in the example which follows (fig. 7.3). The stars indicate the actual measured values. The interpolated values are connected by straight lines, but due to their closeness they give the appearance of a smooth, continuous curve.

7. Example

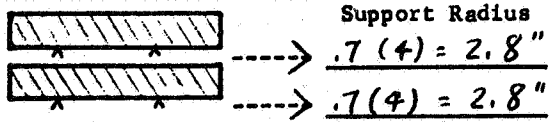
The following example is presented in order to illustrate the calibration process. An eight inch single surface test flat identified as L9210 was calibrated along its A-B and C-D diameters. As given in section 5.2, the flat was supported on top of the NBS 10.6 inch master with both sets of support pads being placed at a radius of 0.70 (4 inches) = 2.8 inches. This necessitated using the empirically derived bending corrections of the master flat for this support radius. Three cycles of measurements were made per run at 11 positions along each diameter. A sample data sheet for one run is given in figure 7.1. The data reduction process was then carried out as shown below where the step numbers correspond to those given in figure 7.2.

<u>Step</u>	<u>Operation</u>	<u>Reference</u>
(1)	Choose positions along x axis	sec. 3.2.
(2)	Compute sum of upper and lower flat profiles (in microinches) for runs I and II from mathematical model	sec. 5.5., 5.6. (eq. 5-11 & 5-18)
(3)	Compute s_I and s_{II} for the two runs	(eq. 5-14)
(4)	Compute (run I profile)-(run II profile)	(eq. 5-19)
(5)	Compute residuals from straight line fit	(eq. 5-23)
(6)	Compute s_t for straight line fit	(eq. 5-24)
(7)	Compute the ratio $s_t^2 / (s_I^2 + s_{II}^2)$	(eq. 5-26)
(8)	Obtain $F_{.99}$ value from table B	(eq. 5-27)
(9)	If good F test, compute mean of profiles from two runs	(eq. 5-28)

OPTICAL FLAT CALIBRATION - 1 FLAT VS. MASTER

Side	Diameter	Run	Test Flat Lot # <u>L9210</u>	Comments: <u>9:10 A.M.</u>
1 T	<u>(A-B)</u>	<u>(1)</u>	Observer <u>E. Erber</u>	
2 <u>(B)</u>	C-D	2	Date <u>4/2/74</u>	

8 Inch Test Flat # L9210
10.6 Inch Master Flat # 1-3
 Test Flat on: (top) bottom



Do not pause during a cycle. OK to pause between cycles.

#	Pos. (inches)	Cycle 1		Cycle 2		Cycle 3		Cycle 4	
		↓	↑	↓	↑	↓	↑	↓	↑
1	<u>1/16"</u>	<u>353</u>	<u>347</u>	<u>346</u>	<u>348</u>	<u>350</u>	<u>347</u>	—	—
2	<u>1/2"</u>	<u>347</u>	<u>342</u>	<u>344</u>	<u>338</u>	<u>344</u>	<u>334</u>	—	—
3	<u>1 1/2"</u>	<u>327</u>	<u>322</u>	<u>321</u>	<u>318</u>	<u>321</u>	<u>315</u>	—	—
4	<u>2 1/2"</u>	<u>298</u>	<u>291</u>	<u>288</u>	<u>282</u>	<u>284</u>	<u>283</u>	—	—
5	<u>3 1/2"</u>	<u>276</u>	<u>271</u>	<u>264</u>	<u>266</u>	<u>261</u>	<u>267</u>	—	—
6	<u>4"</u>	<u>259</u>	<u>253</u>	<u>245</u>	<u>242</u>	<u>244</u>	<u>246</u>	—	—
7	<u>4 1/2"</u>	<u>226</u>	<u>223</u>	<u>219</u>	<u>214</u>	<u>212</u>	<u>208</u>	—	—
8	<u>5 1/2"</u>	<u>154</u>	<u>157</u>	<u>147</u>	<u>145</u>	<u>148</u>	<u>145</u>	—	—
9	<u>6 1/2"</u>	<u>112</u>	<u>113</u>	<u>110</u>	<u>102</u>	<u>99</u>	<u>97</u>	—	—
10	<u>7 1/2"</u>	<u>55</u>	<u>51</u>	<u>40</u>	<u>41</u>	<u>34</u>	<u>33</u>	—	—
11	<u>7 15/16"</u>	<u>35</u>	<u>27</u>	<u>20</u>	<u>23</u>	<u>17</u>	<u>18</u>	—	—
12	—	—	—	—	—	—	—	—	—
13	—	—	—	—	—	—	—	—	—
14	—	—	—	—	—	—	—	—	—
15	—	—	—	—	—	—	—	—	—
16	—	—	—	—	—	—	—	—	—
17	—	—	—	—	—	—	—	—	—
18	—	—	—	—	—	—	—	—	—
19	—	—	—	—	—	—	—	—	—
20	—	—	—	—	—	—	—	—	—
21	—	—	—	—	—	—	—	—	—
22	—	—	—	—	—	—	—	—	—
23	—	—	—	—	—	—	—	—	—

Are the end positions in the dubbing? (yes) no

Compute Fringe Separation
 Fringe 1: 280 271 277 —
 Fringe 2: 68 61 63 —
 Difference: 212 210 214 —
 Average Difference: 212.0

Figure 7.1

A-B Diameter

(1)	(2)	(2)	(4)	(5)	(9)	(10)	(11)	(12)	(14)	(16)
Pos	a _I	a _{II}	z	d	a	a ^M	a ^T	*a ^T	s _a ^{*T}	3s _a ^{*T} +E
.06	19.18	8.47	10.71	.02	13.82	.01	13.81	-2.10	.048	.34
.50	18.82	8.74	10.08	.01	13.78	.12	13.66	-1.54	.031	.29
1.50	17.72	9.05	8.68	.04	13.39	.21	13.18	-.41	.034	.30
2.50	15.97	8.70	7.27	.07	12.33	.21	12.12	.15	.036	.31
3.50	14.91	9.16	5.75	-.02	12.04	.35	11.69	1.32	.037	.31
4.00	13.88	8.87	5.00	-.05	11.38	.34	11.04	1.48	.037	.31
4.50	12.20	7.95	4.25	-.09	10.07	.32	9.75	.99	.037	.31
5.50	8.55	5.74	2.81	-.10	7.15	.27	6.88	-.26	.036	.31
6.50	6.20	4.69	1.51	.04	5.45	.32	5.12	-.41	.034	.30
7.50	2.80	2.73	.07	.02	2.77	.16	2.60	-1.32	.031	.29
7.94	1.78	2.30	-.52	.07	2.04	.06	1.98	-1.23	.048	.34

(3) $s_I = .144$ (6) $s_t = .148$ (13) $s_p = \sqrt{\frac{[(.144)^2 + (.135)^2 + (.132)^2 + (.136)^2]}{4}} = .137$
 $s_{II} = .135$

(7) $\frac{s_t^2}{s_I^2 + s_{II}^2} = \frac{.0219}{.0390} = 0.56$ $E_W = .025 \mu''$

(15) $E_M = .174 \mu''$

(8) $F_{.99}(9,90) = 2.62$ $E = .199 \mu''$

C-D Diameter

Pos	a _I	a _{II}	z	d	a	a ^M	a ^T	*a ^T	s _a ^{*T}	3s _a ^{*T} +E
.06	9.15	9.74	-2.59	.07	10.44	.01	10.43	-1.33	.048	.34
.50	9.09	9.89	-2.81	-.07	10.49	.12	10.37	-.96	.031	.29
1.50	8.74	9.56	-2.82	.10	10.15	.21	9.94	-.39	.034	.30
2.50	7.79	8.93	-3.14	-.04	9.36	.21	9.15	-.19	.036	.31
3.50	7.92	9.18	-3.26	.02	9.55	.35	9.20	.84	.037	.31
4.00	7.71	9.12	-3.41	-.04	9.42	.34	9.08	1.22	.037	.31
4.50	6.92	8.36	-3.43	.03	8.64	.32	8.31	.95	.037	.31
5.50	4.67	6.46	-3.79	-.15	6.56	.27	6.30	-.08	.036	.31
6.50	3.40	5.34	-3.94	-.11	5.37	.32	5.05	-.34	.034	.30
7.50	1.44	3.55	-4.11	-.11	3.49	.16	3.33	-1.06	.031	.29
7.94	1.03	2.83	-3.80	.29	2.93	.06	2.87	-1.08	.048	.34

$s_I = .132$ $s_t = .321$

$s_{II} = .136$

$\frac{s_t^2}{s_I^2 + s_{II}^2} = \frac{.1030}{.0359} = 2.87^*$

*The runs were not repeated even though this number exceeds the maximum F ratio 2.62. There was apparently a bad reading in the dubbing area at the 7.94 position on the x axis as indicated by the value of .29 in the "d" column.

Figure 7.2

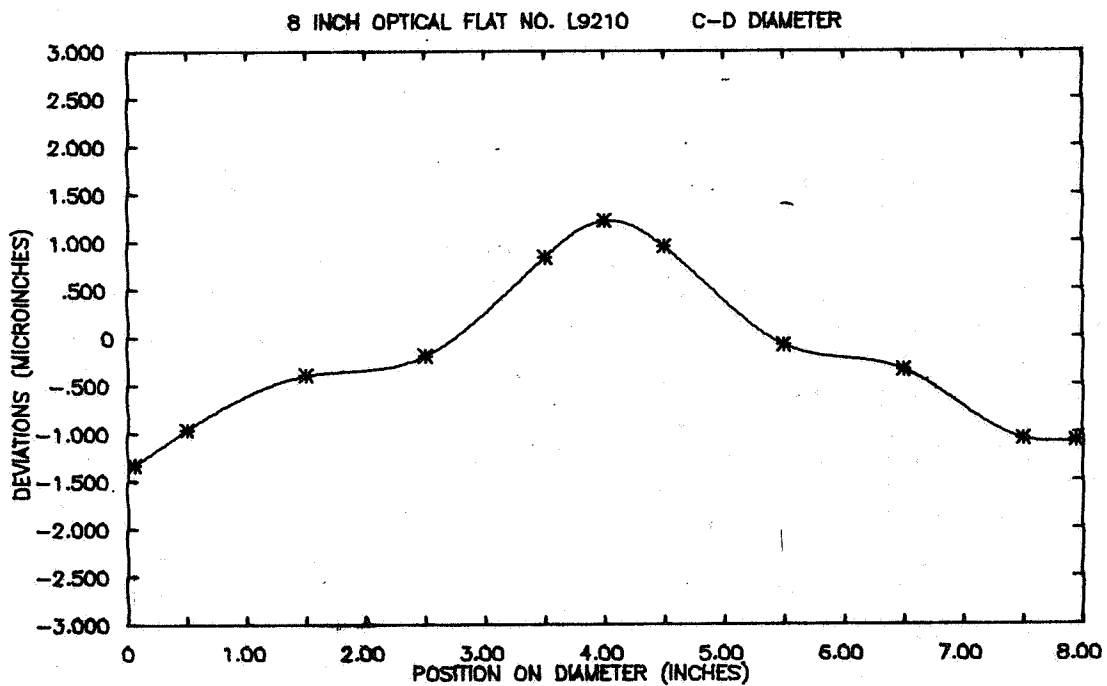
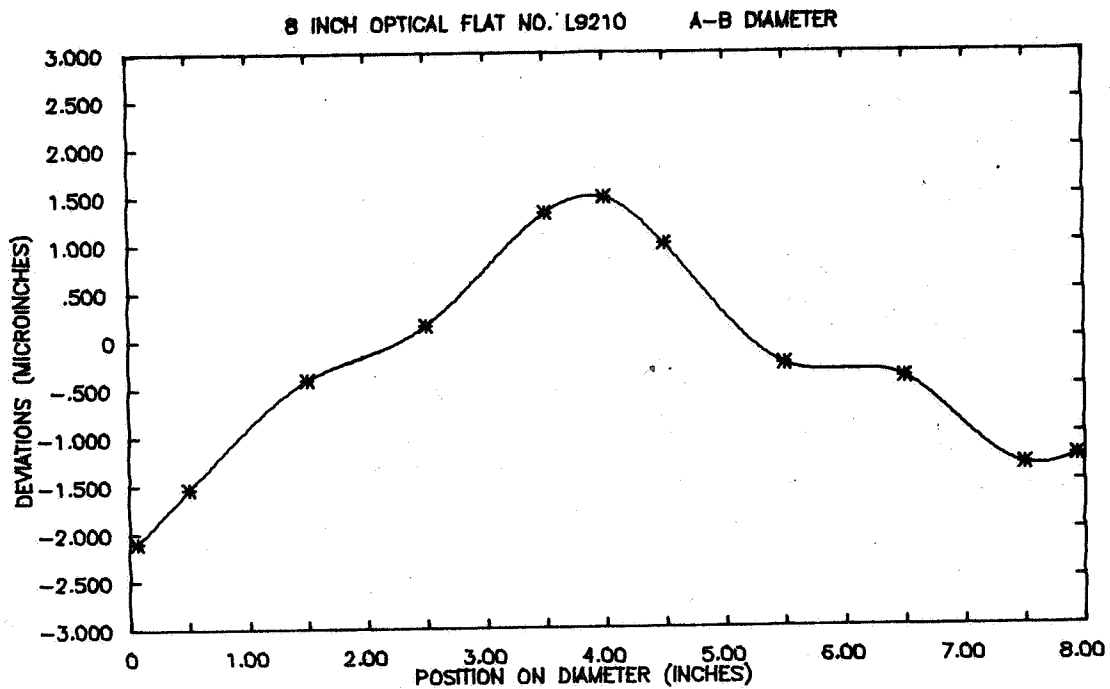


Figure 7.3

- (10) Obtain profile values for master flat
- (11) Subtract master profile from mean profile (eq. 5-30)
- (12) Compute final profile values relative to least squares line (eq. 5-33)
- (13) Compute pooled standard deviation of single measurement sec. 5.7.
- (14) Compute standard deviation of final profile values (eq. 5-38)
- (15) Compute limits for systematic error sec. 5.7. (eq. 5-39 & 5-40)
- (16) Compute total uncertainty for final values (eq. 5-41)

A smooth curve was fit to each set of values in step (12) by the method described in section 6. The graphs are given in figure 7.3.

8. Conclusion

The data reduction part of the calibration process is now fully computerized. The output includes the usual Report of Calibration plus a plot of the profile of each diameter.

There are a couple of pitfalls to be avoided in using the calibrated flat. First, the values on the Report of Calibration are valid only when the flat is supported in the exact manner as it was during calibration. If the flat is supported in a different manner (such as a ring support around the edge) then it will distort to some extent due to gravitational bending. In that case the user must determine the bending corrections for himself unless he chooses to ignore them. Second, if the flat is properly supported on three pads as described in sections 3.1., 4.2., and 5.2. then minimum bending occurs only along those diameters which are parallel to the lines which connect the pads. This means that in the usual case where the A-B and C-D diameters are perpendicular the reported values cannot be legitimately used simultaneously. This is illustrated in figure 8.1. One method of overcoming this difficulty would be to measure the profile along diameters A-B, C-D, and E-F which are 60° apart as shown in figure 8.2.

The main weakness of this calibration process is that it is more "one-dimensional" than "two-dimensional". (An example of a true two-dimensional calibration using an entirely different technique is given by Dew [2].)

BENDING PROPERTIES FOR .70R SUPPORT

A—B MINIMUM BENDING
C—D NOT MINIMUM BENDING

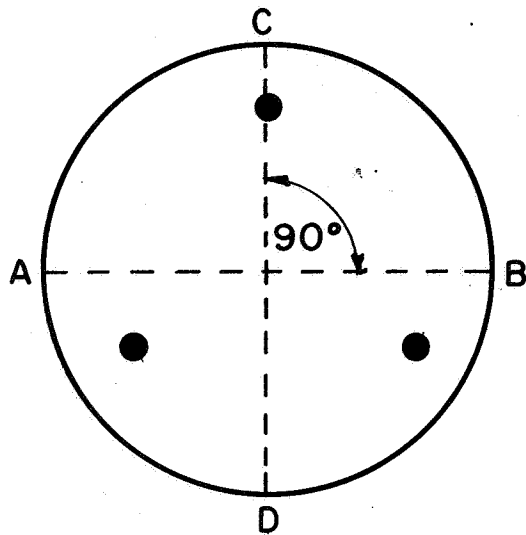


Figure 8.1

A—B, C—D, E—F MINIMUM BENDING

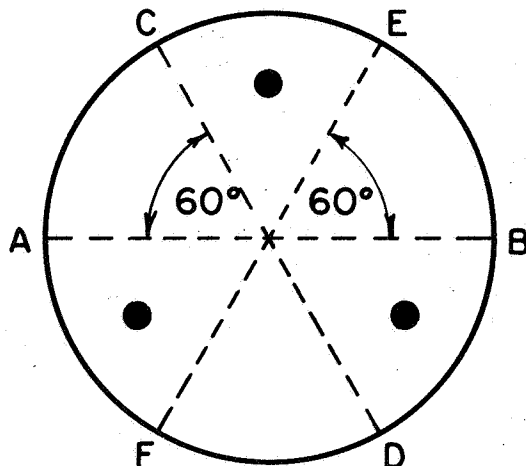


Figure 8.2

Despite this shortcoming, the process does give a high degree of measurement accuracy and it has sufficiently met the needs of a large number of optical flat users for many years.

I wish to acknowledge three people who were of great assistance to me in the writing of this paper. I thank Mr. Ralph C. Veale of the Dimensional Technology Section who spent much time acquainting me with the many facets of this complex measurement process. I also thank Mr. Joseph M. Cameron of the Office of Measurement Services for his many helpful suggestions on improving the paper. Finally, I thank Dr. James J. Filliben of the Statistical Engineering Laboratory for suggesting the mathematical model and statistical test which appear in sections 5.5. and 5.6.

Table A. Guide for setting up flats

Test flat diameter	Test flat position	Which master?	Master support radius	Apply master bending corr.?
0" - 7"	top	10.6"	$.70r_M$	no
7" - 10.6"	top	10.6"	$.70r_T$	yes
12"	either	12.25"	$.70r_T$	*
16"	either	16"	$.70r_T$	*

Odd sizes over 10.6" are calibrated either by overlapping or by a 3-flat comparison with two other flats of the same size. The method of overlapping involves calibrating the central segment and the two end segments separately and then fitting them together.

* Test flat diameter may vary slightly from master flat diameter. Since bending values are not known for these two master flats, an error term must be added to the master flat uncertainty if its support radius is not exactly $.70r_M$.

Table B. Percentiles of the F distribution

Values of $F_{.99}(n-2, 4mn-2n-8m+4)^*$ for certain m and n

n	m			
	1	2	3	4
5	9.78	5.09	4.51	4.29
6	7.01	4.22	3.83	3.67
7	5.64	3.70	3.41	3.29
8	4.82	3.35	3.12	3.03
9	4.28	3.10	2.91	2.82
10	3.89	2.90	2.74	2.67
11	3.60	2.76	2.62	2.56
12	3.37	2.63	2.51	2.46
13	3.18	2.53	2.42	2.37
14	3.03	2.44	2.34	2.30
15	2.91	2.37	2.28	2.23
16	2.80	2.31	2.21	2.18
17	2.70	2.25	2.16	2.13
18	2.62	2.20	2.11	2.09
19	2.55	2.16	2.07	2.06
20	2.49	2.12	2.03	2.02
21	2.43	2.08	2.00	1.99
22	2.37	2.04	1.97	1.95
23	2.33	2.01	1.94	1.92
24	2.28	1.99	1.92	1.90
25	2.24	1.97	1.90	1.88

*Values taken from the twelfth edition of C.R.C. Standard Mathematical Tables, with some interpolation.

References

- [1] Ahlberg, J. H., Nilson, E. N., and Walsh, J. L., The Theory of Splines and Their Applications, Academic Press, 1967, section 2.1.
- [2] Dew, G. D., The Measurement of Optical Flatness, Journal of Scientific Instruments, Vol. 43, pp. 409-415, 1966.
- [3] Dew, G. D. Systems of Minimum Deflection Supports for Optical Flats, Journal of Scientific Instruments, Vol. 43, pp. 809-811, 1966.
- [4] Emerson, Walter B., Determination of Planeness and Bending in Optical Flats, Journal of Research of the National Bureau of Standards, Vol. 49, No. 4, pp. 241-247, October 1952.
- [5] Timoshenko, S., and Woinowski-Krieger, S., Theory of Plates and Shells, 2nd Edition, McGraw-Hill Book Co., 1959, sections 20 and 65.
- [6] UNIVAC, MATH-PACK Programmers Reference, Sperry Rand Corporation, 1970, pp. 2-68 through 2-72.